Study on the Crystallization Kinetics of PP/GF Composites

HORNG-JER TAI, WEN-YEN CHIU, LEO-WANG CHEN, and LINE-HWA CHU

Department of Chemical Engineering, National Taiwan University, Taipei, Taiwan, Republic of China

SYNOPSIS

The crystallization kinetics and morphology of glass fiber-reinforced polypropylene (PP/GF) were investigated in this work. Both isothermal and nonisothermal crystallization behaviors of 90PP/10GF, 80PP/20GF, and 70PP/30GF were examined with a DSC instrument. It was found that the addition of glass fiber would increase the crystallization rate of PP and increase the content of β spherulite, which was most likely formed at temperatures between 390 and 400 K. The morphology of spherulites of PP/GF composites were examined with SEM and a polarized microscope. All experimental observations conformed rather well with the theoretical approach, a dynamic crystallization model, proposed in our previous work. The size of α spherulites of PP would decrease at lower crystallization temperature, or at higher cooling rate, or by adding glass fiber in it.

INTRODUCTION

PP is a kind of crystalline polymer, in which three forms of crystal structures α, β, and γ forms[1] have been found. Mostly, the α (monoclinic) form dominates the crystalline phase of PP. However, if hetero nuclei[2] exist or quick cooling[3] is imposed on the sample, we could find the β (hexagonal) form structure.[4] Also, the γ (triclinic) form structure could be found in the case of extremely high pressure. The spherulites of PP include I, II, III, IV, and mixed types.[5] The I, II, and mixed types mainly have the structure of the α form, whereas the III and IV types mainly have the structure of the β form. Each spherulite may differ from others either in the lamella coordination or in shapes. The crystallization kinetics of PP was thoroughly studied in our previous work.[6] However, the study on the crystallization kinetics of fiber-reinforced plastics was rather few. Velisaris and Seferis[7] examined the crystallization kinetics of the PEEK/carbon fiber system, in which the crystallization rate and crystallinity were found to be lower than the pure PEEK polymer. Lee and Porter[8] investigated the crystallization behavior for the same system. They indicated that a higher nucleation density was distributed along carbon fibers. The crystallization rate increased with increasing the content of carbon fiber under nonisothermal cooling. Meanwhile, a transcrystalline structure was found on the interface of the carbon fiber and polymer matrix. Jog and Nadkarni[9] found an increase of crystallization rate, but a decrease of crystallinity with glass fiber in PPS. Campbell and Qayyum[10] observed the crystal growth with several kinds of fibers in PP. He found that the addition of fibers would increase the nucleation density. The transcrystalline structure would form on the interface of fiber and PP if the fiber was nylon, terylene, kevlar, or carbon fiber. Gupta et al.[11] utilized a DSC instrument to measure the crystallization rate of the PP/glass fiber system under nonisothermal cooling. It was found that both the crystallinity and crystallization rate of PP increased with the addition of glass fiber, and the size distribution of spherulites tended to be sharper.

In this work we adopted the similar approach as in our previous work[6] to analyze the crystallization kinetics of the PP/glass fiber system. The crystallization rate constant, size of spherulites, and nucleation density at isothermal and nonisothermal cooling were investigated.

THEORETICAL CONSIDERATION

The crystallization mechanism of PP was shown to be of instantaneous nucleation and spherical growth

Journal of Applied Polymer Science, Vol. 42, 3111–3122 (1991)
 CCC 0021-8995/91/123111-12$04.00

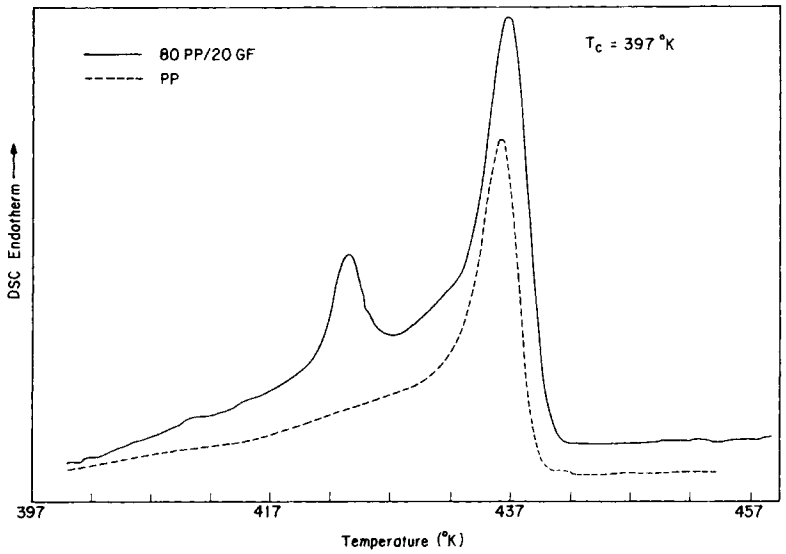

Figure 1 DSC thermogram for the melting of PP and GFRPP that crystallized at 397 K. (———) 80 PP/20 GF; (· · · · · · · · ·) PP.

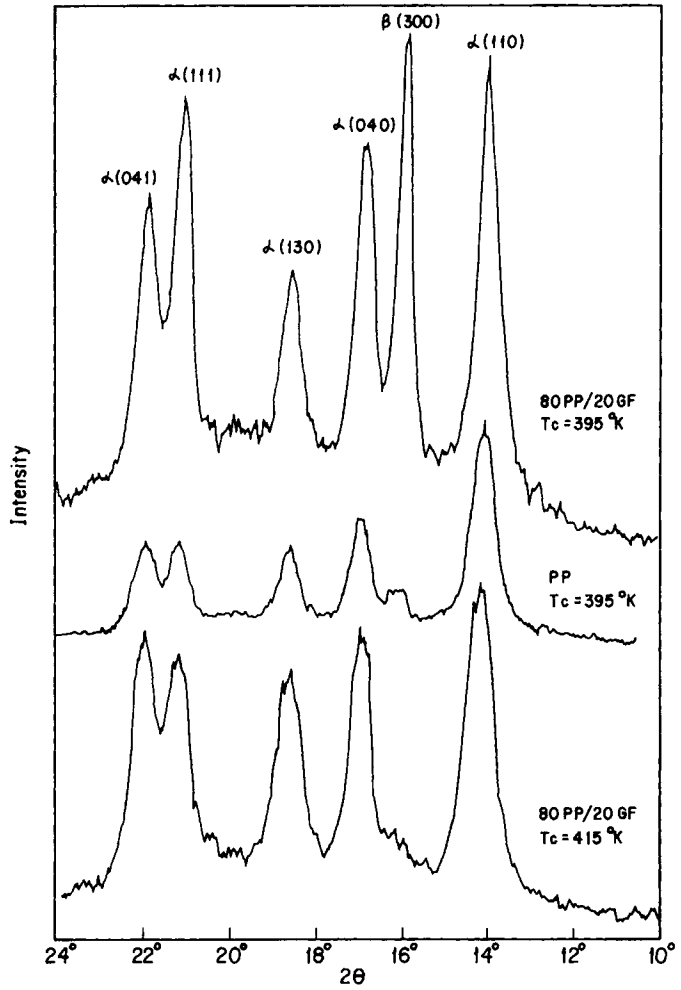

Figure 2 X-ray diffraction diagram of PP crystalline forms using CuK_α radiation. The notations above each diffraction peaks are the corresponding crystal form and miller index.

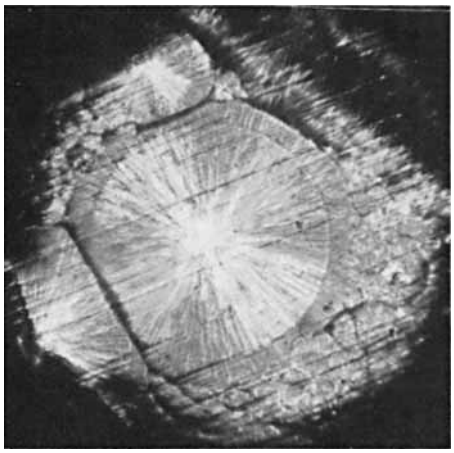

(a) PP, Tc=407°K, Time=1.0 hr

Observed radius 139 μm

(b) PP, Tc=407°K, Time=2 hr

Observed radius 270 μm

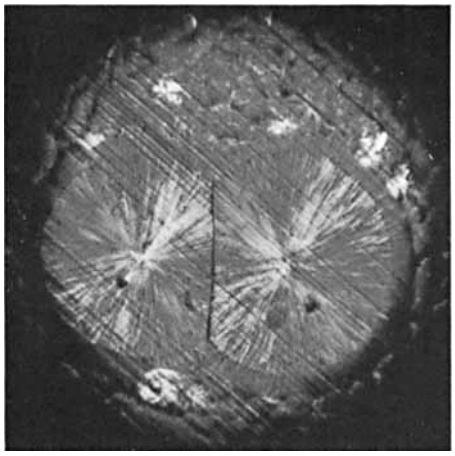

(c) PP, Tc=410°K, Time=1.5 hr

Observed radius 110-130 μm

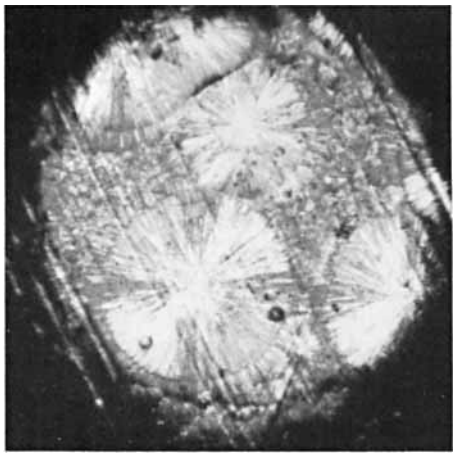

(d) 90PP/10GF, Tc=410°K, Time=1.5 hr

Observed radius 90-120 μm

Figure 3 Isothermally growing spherulites observed under polarized microscope. Scale bar = 100 μm.

Table I Growth Rate of α Spherulites at Various Crystallization Temperatures

T_c (K)	G (1·E − 5 mm/s)
393	37.7
395	27.3
399	17.
401	9.29
403	8.465
405	7.023
407	4.447
410	2.214
413	1.53
415	.9546

in crystals.[6] The basic equations for the relative crystallinity (x_r) of PP, the concentration of spherulites (N), the growth rate of spherulites (G), and the crystallization rate constant (K) at isothermal and nonisothermal conditions were derived in our previous work,[6] which are summarized in the appendix of this paper.

The average radius of spherulites was estimated to lie between two bounds, R^l_{av} and R^u_{av}:

$$R^l_{av} = (3dX_c/4\pi N_t d_c)^{1/3} \quad (1)$$

$$R^u_{av} = (3/4\pi N_t)^{1/3} \quad (2)$$

where N_t was the concentration of spherulites, X_c was the absolute crystallinity, d_c was the density of crystalline phase, and d was the apparent density of sample.

Equation (1) was derived under the assumption of 100% crystallinity in spherulites. It underestimated the size of spherulites; hence, R^l_{av} was the lower bound of the radius of spherulites, whereas eq. (2) was derived under the assumption of full mixing between amorphous phase and crystalline phase. In other words, the amorphous regions were totally incorporated and distributed in spherulites. It overestimated the size of spherulites; hence, R^u_{av} was the upper bound of the radius of spherulites.

EXPERIMENTAL

Materials

1. PP, M.I. = 3.0 g/10 min.
2. Glass fiber, 6 mm; chopped strand, 5–22 μm in diameter; sp gr = 2.61.

Preparation of Specimens

PP and glass fiber were mixed and blended through an extruder to form a composite (GFRPP). The screw speed was set at 25 rpm, and the temperatures of three zones of extruder were set at 200, 210, and 220°C. The extrudate was then cut and hot pressed under 220°C and 250 kg/cm^2 to prepare thin sheets. The thin sheets were well cut to prepare the specimens for the DSC test, in which the sample containing 90 wt % PP and 10 wt % GF was designated 90 PP/10 GF, and others were designated in a similar way.

Isothermal Crystallization Experiments

In isothermal crystallization experiments, the specimen was heated at 493 K for 10 min in order to completely eliminate the crystal structure. Then, it was quenched down by the rate of 320 K/min to the set crystallization temperature. The range of crystallization temperature was selected from 387 to 405 K in our experiments. The exothermic curve during the crystallization process could be read from the DSC recorder. After about 30 min, the specimen in DSC was again heated by the rate of 10 K/min to 493 K, and its melting curve could also be read from the DSC recorder.

Nonisothermal Crystallization Experiments

In nonisothermal crystallization experiments, the specimen was first heated at 493 K for 10 min. Then,

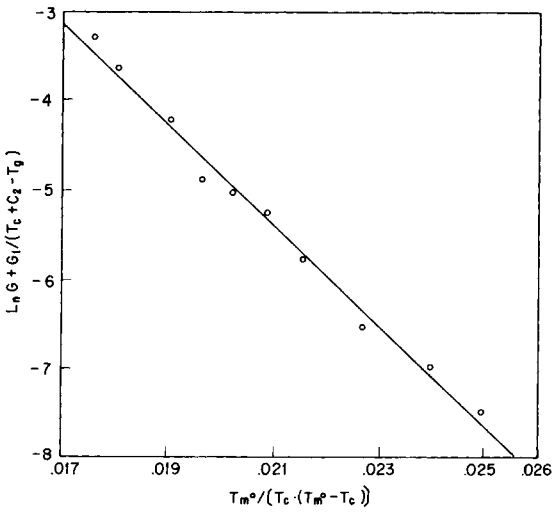

Figure 4 Growth rate of α spherulites correlating to temperature by using eq. (a-3) with parameters listed in Table IIA.

Table II Parameters for Equations

A. Parameters for Eqs. (a-2), (a-3) and (a-4) of Pure PP

						Max. T^a
ln G_0	8.346	G_1	−750.	G_2	−569.6	355 K
ln K_0	63.81	K_1	−2704.	K_2	−2834.	347 K
ln N_0	37.34	N_1	−454.	N_2	−1128.	326 K
T_m^0	459.4 K	C_2	30 K	T_g	260 K	—

B. Parameters for Eqs. (a-3), (a-4), and (3) of GFRPP

	90PP/10GF	80PP/20GF	70PP/30GF
a[b]	.66591	.8367	.891
ln K_0	64.534	64.324	64.261
ln N_0	38.064	37.854	37.791

G_1 from Ref. 12; K_1 from Ref. 13, C_2, T_g from Ref. 14. G in (cm/min); K in (min^{-3}), N in (cm^{-3}).
[a] Temperature for maximum K, G, and N, respsectively.
[b] $t_{1/2}$ (GFRPP) = $a \cdot t_{1/2}$ (PP).

it was cooled down by the rate of 2.5, 5, 10, 20, or 40 K/min to 325 K. Afterward, it was immediately heated by the rate of 10 K/min to 493 K. The crystallization curve and the corresponding melting curve were recorded.

Morphology Observation

The observation of morphology of specimens during the crystallization process was done with SEM and a polarized microscope. The growth and the sizes of spherulites were carefully examined.

RESULTS AND DISCUSSION

α and β Spherulites

Figure 1 showed the DSC melting curves of PP and 80PP/20GF, which crystallized at 397 K. It was found that the addition of fiber in PP would induce

Table III Values of $t_{1/2}$ and K for PP and GFRPP Under Isothermal Crystallization Experiments

	PP		90PP/10GF	
T_c	$T_{1/2}$	K	$t_{1/2}$	K
K	min	min^{-3}	min	min^{-3}
387.0	.6450	.1501E + 01	.598	.2730E + 01
389.0	.9890	.6762E + 00	.876	.9321E + 00
390.0				
391.0	1.600	.2096E + 00	1.272	.3212E + 00
392.0				
393.0	2.291	.5769E − 01	1.749	.1127E + 00
395.0	3.478	.1588E − 01	2.639	.3686E − 01
396.0				
397.0	4.834	.6116E − 02	4.097	.9555E − 02
398.0				
399.0	8.656	.1247E − 02	5.870	.3254E − 02
401.0	12.41	.3655E − 03	8.555	.1092E − 02
403.0	19.89	.1537E − 03	13.41	.2720E − 03
405.0	26.74	.3452E − 04	17.27	.1250E − 03

$t_{1/2}$: crystallization half-time; K: obtained by fitting the Avrami equation $Xr = 1 - \exp(-K \cdot t^{-3})$.

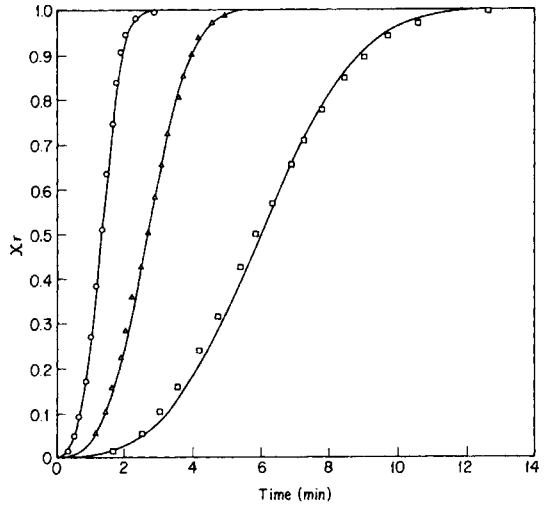

Figure 5 Relative crystallinity of 90 PP/10GF as function of time at different temperatures. Experimental: (○) T_c = 391 K; (△) T_c = 395 K; (□) T_c = 399 K; (———): Predicted by Avrami equation $X_r = 1 - \exp(-K \cdot t^{-3})$.

the β spherulite (mp = 418–433 K) in addition to the α spherulites (mp = 430–455 K) in pure PP. This phenomenon was also confirmed in the X-ray diffraction diagram, which is shown in Figure 2. When the crystallization temperature was between 390 and 400 K, β spherulites could be found to coexist with α spherulites. The fiber in PP could increase the content of β spherulites.

Growth Rate of Spherulites

The β spherulites usually formed at lower temperature; the growth rate of it was not easy to determine accurately. In this work, the β spherulites were minor; therefore, the measurement of the growth rate of spherulites was mainly based on the α spherulites. The growth rates of α spherulites of PP and GFRPP were functions of temperature. From our observation of morphology of the above specimens with a polarized microscope during the crystallization process, the radii of growing spherulites at different crystallization temperatures were measured and are shown in Figure 3. The average growth rate of α spherulites under different temperatures were then calculated and are listed in Table I. It was seen that the growth rate (G) decreased with increasing the crystallization temperature within our experimental conditions. Since the value of G for PP could be correlated by eq. (a-3), Figure 4 showed the plot of $\ln G + G_1/(T_c + C_2 - T_g)$ vs. $T_m^0/T_c\Delta T$, from which the parameters, G_0 and G_2, were obtained and are listed in Table IIA. The greatest growth rate of spherulites

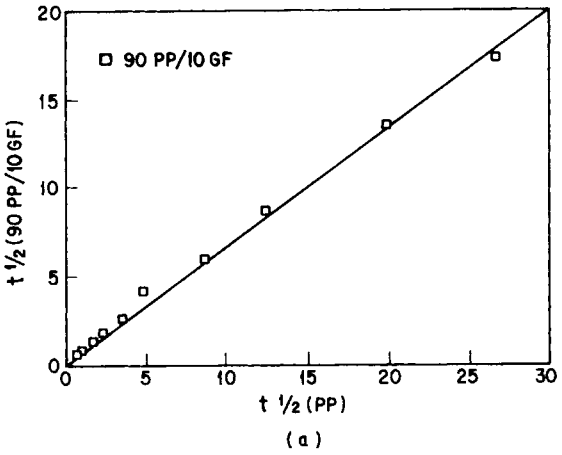

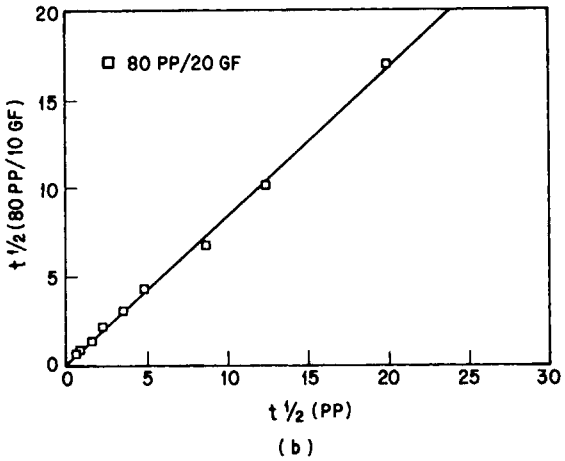

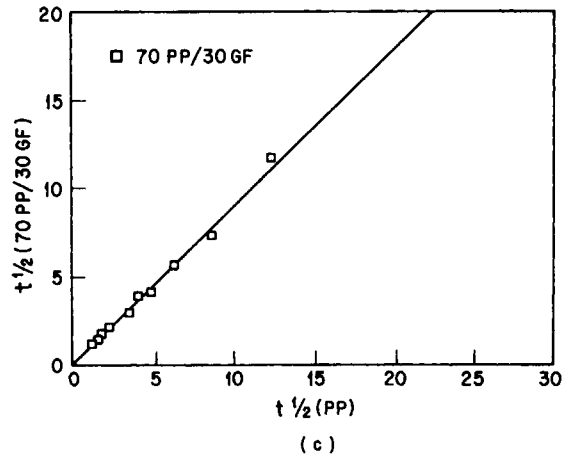

Figure 6 Crystallization half-time correlation. These lines can be correlated by $t_{1/2} = a \cdot t_{1/2}$ (PP) with parameter, a, listed in Table IIB. (a) 90 PP/10GF; (b) 80PP/20GF; (c) 70PP/30GF.

Table IV Absolute Crystallinity Under Isothermal Crystallization Experiments

	Crystallinity[a]	
T_c (K)	PP	90PP/10GF
387	.455	.463
389	.458	.453
391	.458	.458
393	.460	.459
395	.460	.463
397	.464	.471
399	.463	.474
401	.473	.474
403	.474	.474

[a] Take 50 cal/g as heat of fusion of perfect crystalline PP.

would occur at 355 K from the computation of eq. (a-3).

Isothermal Crystallization Kinetics

The relative crystallinity $X_r(t)$ of the sample could be calculated from the integration of the isothermal crystallization–exotherm curve of DSC (i.e., $(dH)/(dt)$ vs. t) according to the following equation[6]:

$$X_r(t) = \frac{\int_0^t \left(\frac{dH}{dt}\right)dt}{\int_0^\infty \left(\frac{dH}{dt}\right)dt} \qquad (3)$$

Rearranging the Avrami equation by taking the double logarithm at both sides of eq. (a-1), we got

$$\ln[-\ln(1 - X_r)] = \ln K + n \ln t \qquad (4)$$

The best values of K and n were obtained from least mean square fitting DSC data to eq. (4). The values of n varied randomly with T_c for PP or GFRPP, but all were close to 3. For simplicity, the value of n was fixed as 3 and the corresponding values of K were as listed in Table III. Figure 5 shows the relative crystallinity of 90PP/10GF as function of time at different crystallization temperatures. The experimental data conformed well with the prediction of the Avrami equation with parameters K and n of Table III. It was seen from Table III that the crystallization rate constant (K) was higher at lower T_c within our experimental condition; hence, the crystallization rate increased with decreasing T_c (Fig. 5). The addition of fiber in PP would increase the crystallization rate in the order of 90 PP/10GF > 80 PP/20GF > 70 PP/30GF > PP. The fiber might act as nucleus in this system. However, if the fiber content was high up to 20 wt %, it might hinder the crystal growth of PP; hence, the crystallization rate would be a little bit retarded.

The crystallization half-time ($t_{1/2}$) was defined as the time at which the relative crystallinity was up to 50%. The values of $t_{1/2}$ of GFRPP read from Figure 5 were plotted vs. the $t_{1/2}$ of PP in Figure 6. Good linear relationships were found and could be correlated by the following equation:

$$t_{1/2}^{\text{GFRPP}} = a \cdot t_{1/2}^{\text{PP}} \qquad (5)$$

The proportional constant a for each GFRPP sample

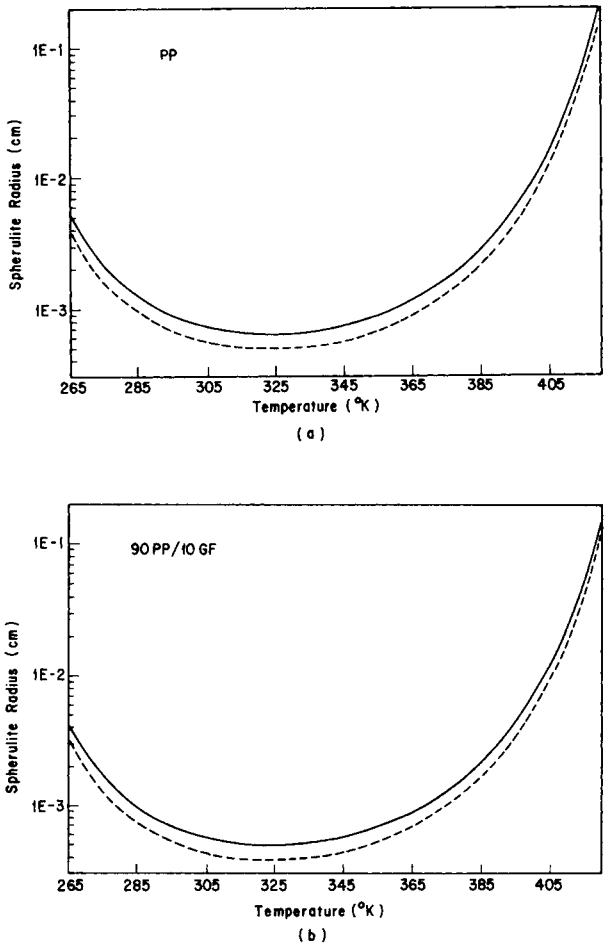

Figure 7 Calculated spherulite radius of PP at various temperatures, when subjected to isothermal crystallization. (a) PP; (b) 90PP/10GF. (———) Upper limit; (· · · · · · · ·) lower limit.

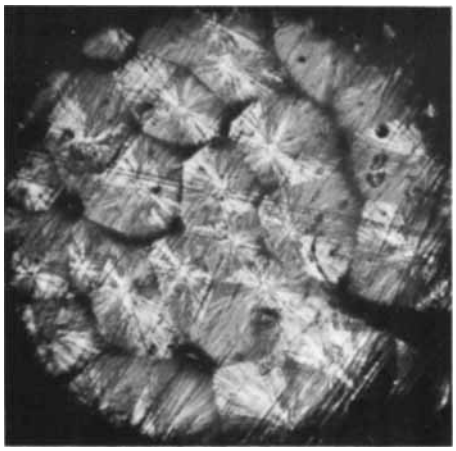

(a) 90PP/10GF, Tc=407 °K

Observed radius 90-160 μm

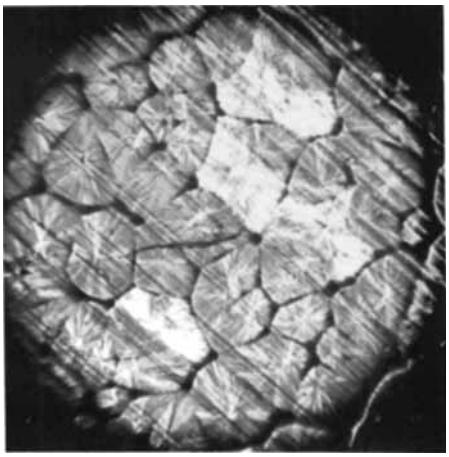

(c) PP, Tc=395 °K

Observed radius 45-120 μm

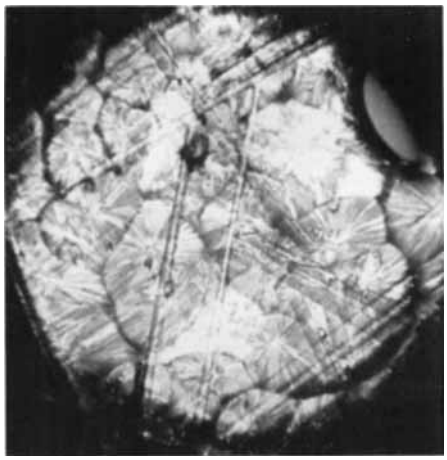

(b) 90PP/10GF, Tc=395 °K

Observed radius 28-75 μm

Figure 8 Pictures of PP and GFRPP spherulites crystallized at different temperatures with predicted mean radius: (a) 140 μm; (b) 50 μm; (c) 54 μm; Scale bar = 100 μm.

is listed in Table IIB. Moreover, the following relation of K and $t_{1/2}$ held:

$$K = \ln 2/t_{\frac{1}{2}}^3 \qquad (6)$$

Therefore, the values of K for each GFRPP could also be estimated from the values of $t_{1/2}$ by eq. (6) and correlated in the form of eq. (a-4) by only adjusting the value of K_0. The values of K_0 for GFRPP

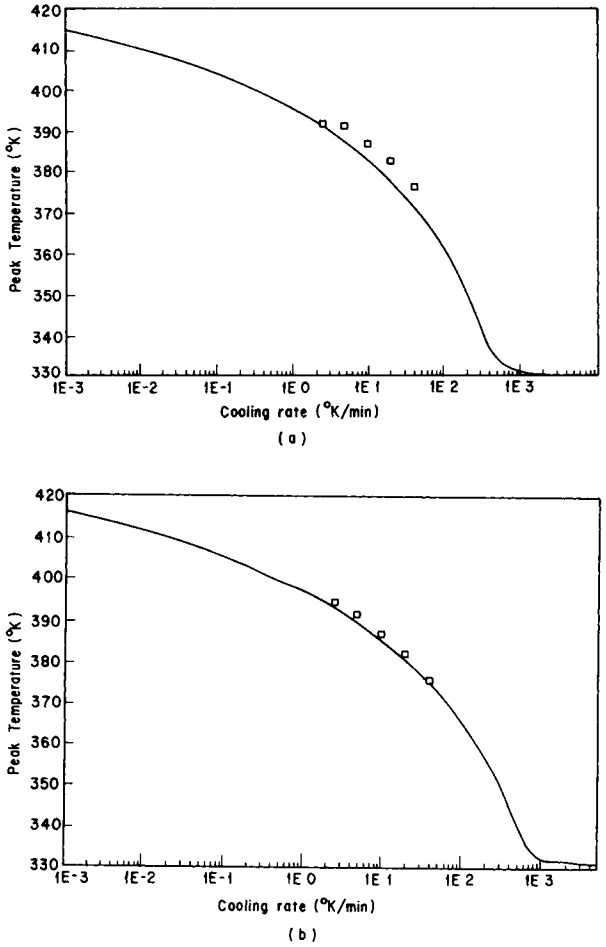

Figure 9 Simulated and experimental peak temperatures of crystallization exotherms: (a) PP; (b) 80PP/20GF. (□) Experimental data; (———) simulated result.

were then obtained very easily and are shown in Table IIB.

Theoretically, the greatest crystallization rate would occur at about 347 K for PP or GFRPP. By using eqs. (a-2), (a-3), and (a-4) and the relation of $K = (4/3)\pi G^3 N$, the concentration of spherulites (N) could be calculated, and the values of N_0, N_1 and N_2 are shown in Tables IIA and IIB. Here, the growth rate of α spherulites was independent of the fiber content, and the variation of N for GFRPP with respect to PP came from the variation of N_0 only. The greatest concentration of spherulites would occur at about 326 K by prediction.

The absolute crystallinity that was obtained from the DSC melting curve[6] under isothermal crystallization experiments vs. T_c is shown in Table IV for both PP and GFRPP. The absolute crystallinity slightly increased with increasing T_c. The values of

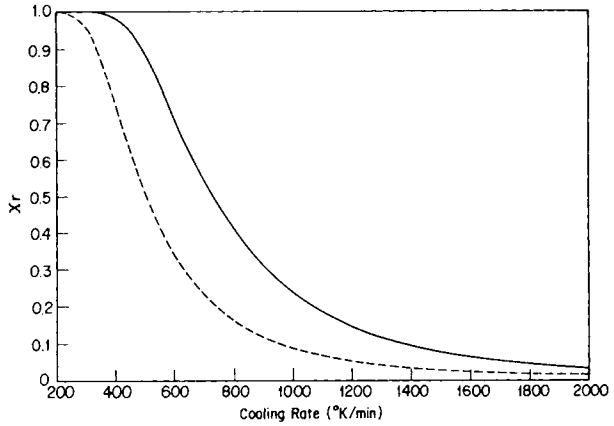

Figure 10 Relative crystallinity as function of cooling rate. (· · · · · · · · ·) PP; (———) 90PP/10GF.

absolute crystallinity were substituted into eqs. (1) and (2) to estimate the lower and upper limit of the radius of spherulites under isothermal crystallization. The calculated values at any T_c were shown in Figure 7 for PP and 90 PP/10GF. The sizes of spherulites for GFRPP were smaller than those of PP, which were rather comparable to the experimental observation of Figure 8.

Nonisothermal Crystallization Kinetics

The nonisothermal crystallization experiments were carried out with DSC at a constant cooling rate. The peak temperatures of crystallization exotherms at different cooling rates are shown in Figure 9 for PP and 80PP/20GF. The temperature at which $dX_r(t)/dt = 0$ was taken as the simulated peak temperature. From the prediction, the peak temperature of crystallization exotherm would all occur at about 330 K when the cooling rate was higher than 1000 K/min. This temperature (330 K) was close to the maximum temperature of nucleation, 326 K in Table IIA. It meant that nucleation was the rate-controlling step during the crystallization process under the condition of quick cooling.

The addition of fiber in PP would slightly increase the peak temperature of crystallization at a low cooling rate, but no significant difference in peak temperature was found between PP and GFRPP at a higher cooling rate. The higher the cooling rate, the lower the peak temperature of crystallization would be for both PP and GFRPP.

Figure 10 showed the predicted relative crystallinity [$X_r(\infty)$ in eq. (a-5)] as a function of cooling rate for PP and 90 PP/10GF. The fiber would in-

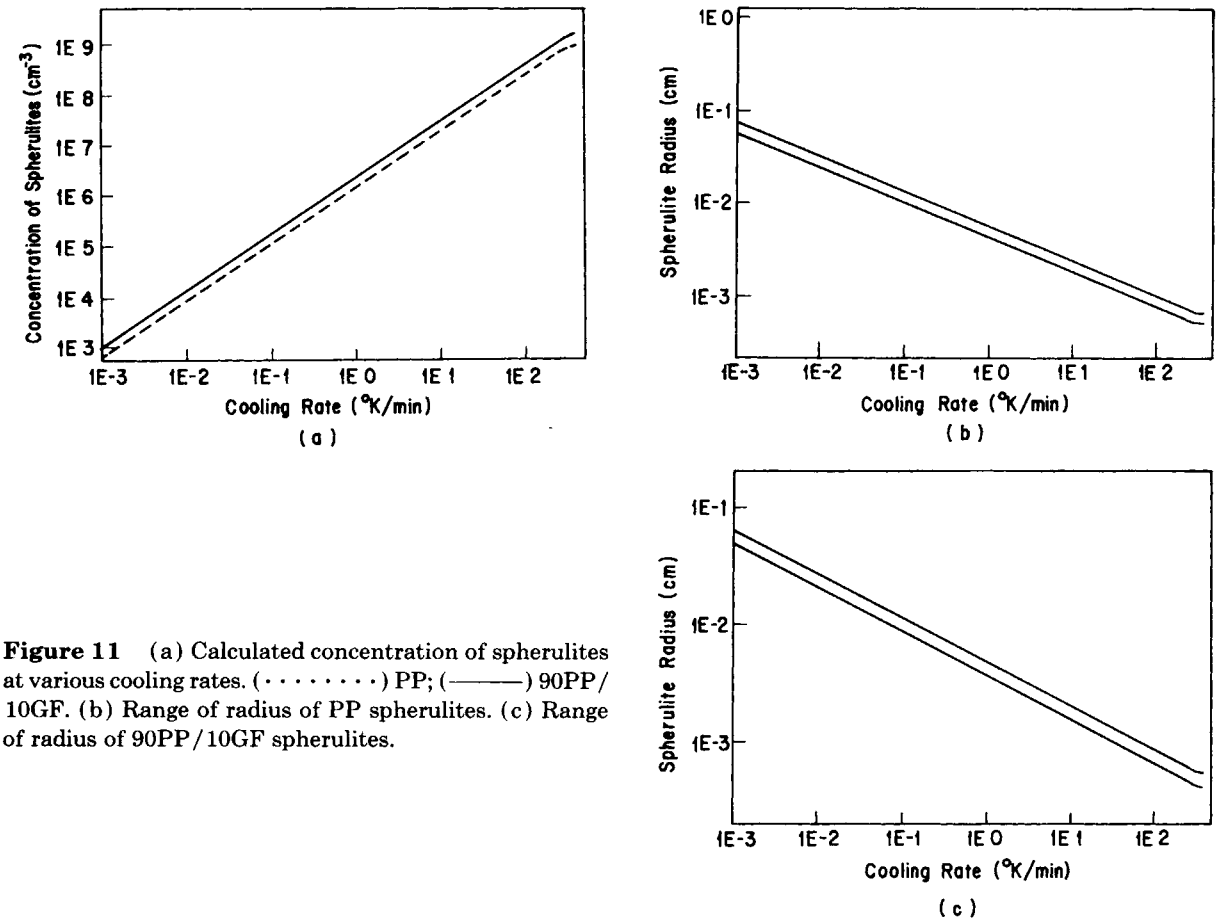

Figure 11 (a) Calculated concentration of spherulites at various cooling rates. (· · · · · · · · ·) PP; (———) 90PP/10GF. (b) Range of radius of PP spherulites. (c) Range of radius of 90PP/10GF spherulites.

crease the crystallization rate of PP as mentioned above in the case of isothermal crystallization. Figure 1(a) shows the calculated concentration of spherulites at various cooling rates for PP and 90PP/10GF by eqs. (a-6) and (a-7). Figures 11(b) and (c) shows the calculated lower and upper limits of the radius of spherulites, respectively [by eqs. (1) and (2)], at various cooling rates for PP and 90PP/10GF. It was seen that the concentration of spherulites was higher at higher cooling rates, but the size of spherulites decreased at higher cooling rates. Also, the radius of spherulites of GFRPP was smaller than that of PP.

Figure 12 shows the observed spherulites of PP and GFRPP under a constant cooling rate with a polarized microscope and SEM. When the cooling rate was lower than 10 K/min, the observed radii of spherulites were slightly larger than were the theoretical calculated ones that are listed in the caption of Figure 12. But when the cooling rate was higher than 10 K/min, an opposite trend was found.

It was concluded that our proposed dynamic crystallization model was good for the prediction of crystallinity, concentration of spherulites, and size of spherulites for PP and GFRPP under both isothermal and nonisothermal crystallization processes.

APPENDIX

Basic Equations for the Crystallization Kinetics of PP

I. At Isothermal Condition

The Avrami equation was used to describe the crystallization kinetics of PP, i.e.,

$$X_r(t) = 1 - \exp(-Kt^n) \qquad \text{(a-1)}$$

where $X_r(t)$ = relative crystallinity of polymer; K = crystallization rate constant; and n = Avrami exponent. The value of n was near 3 and $K = (4/3)\pi G^3 N$, where G was the growth rate of spherulites and N was the concentration of spherulites.

According to our previous work,[6] the following

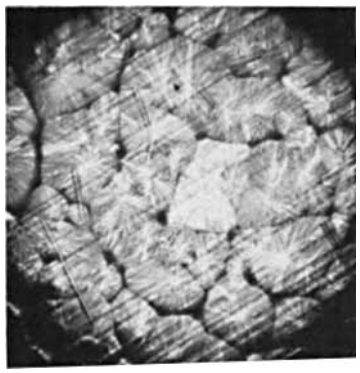

(a) 90PP/10GF 2.5 °K/min (PM)

Observed radius 28-130 μm

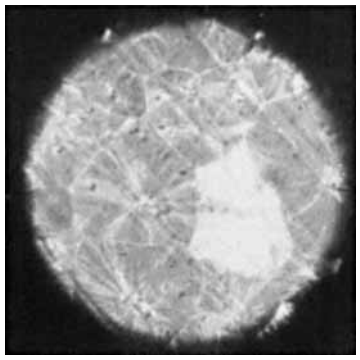

(b) PP, 10 °K/min (PM)

Observed radius 18-60 μm

(c) PP , 40 °K/min (SEM)
Observed radius 2-5 μm

Figure 12 PP and GFRPP spherulites that grew under a constant cooling rate and were observed by a polarized microscope (PM) and SEM. Theoretical calculated mean radius: (a) 33 μm; (b) 25 μm; (c) 13 μm; Scale bar = 100 μm.

equations were obtained:

$$N = N_0 \exp[N_1/(T_c + C_2 - T_g)] \times \exp[N_2 T_m^0/T_c \Delta T] \quad \text{(a-2)}$$

$$G = G_0 \exp[G_1/(T_c + C_2 - T_g)] \times \exp[G_2 T_m^0/T_c \Delta T] \quad \text{(a-3)}$$

$$K = K_0 \exp[K_1/(T_c + C_2 - T_g)] \times \exp[K_2 T_m^0/T_c \Delta T] \quad \text{(a-4)}$$

where $K_0 = (4/3)\pi G_0^3 N$; T_c was the crystallization temperature; T_m^0 was the limiting melting temperature; T_g was the glass transition temperature; $(T_g - C_2)$ was the temperature theoretically at which any movement of chains or segments ceased; and $\Delta T = T_m^0 - T_c$.

II. At Nonisothermal Condition

The relative crystallinity was derived as[6]

$$X_r(t) = X(t)/X_{l0}$$
$$= 1 - \exp\left\{\frac{-4\tau}{3}\int_{t_0}^{t}\left[\int_{\tau}^{t} G(T(u))du\right]^3 \times \left.\frac{dN}{dT}\right|_{T=T(\tau)} \left.\frac{dT}{dt}\right|_{t=\tau} d\tau\right\} \quad \text{(a-5)}$$

where X_{l0} was the limiting absolute crystallinity at zero cooling rate and $X(t)$ was the absolute crystallinity at time t.

The concentration of spherulites was derived as[6]

$$N(t) = \int_0^t \dot{N}(\tau)[1 - X_r(\tau)]d\tau \quad \text{(a-6)}$$

where $\dot{N}(\tau)$ was the nucleation rate at nonisothermal condition, which could be expressed as

$$\dot{N}(\tau) = \left.\frac{dN}{dT}\right|_{T=T(\tau)} \cdot \left.\frac{dT}{dt}\right|_{t=\tau} \quad \text{(a-7)}$$

The growth rate of spherulites, G, followed the form of eq. (a-3), and the relation of $K = (4/3)\pi G^3 N$ held.

REFERENCES

1. A. Turner-Jones, J. M. Aizlewood, and D. R. Beckett, *Macromol. Chem.*, **75,** 134 (1964).
2. P. Jacoby, B. H. Bersted, W. J. Kissel, and C. E. Smith, *J. Polym. Sci. Polym. Phys. Ed.*, **24,** 461 (1986).
3. A. J. Lovinger, J. O. Chua, and C. C. Cryte, *J. Polym. Sci. Polym. Phys. Ed.*, **15,** 641 (1977).
4. H. D. Kieth, F. J. Padden, N. M. Walter, and M. W. Wycoff, *J. Appl. Phys.*, **30,** 1485 (1959).
5. F. J. Padden and H. D. Kieth, *J. Appl. Phys.*, **30,** 1479 (1959).
6. C. C. Fan-Chiang, Master Thesis, National Taiwan University, 1987.
7. C. N. Velisaris and J. C. Seferis, *Polym. Eng. Sci.*, **26,** 1574 (1986).
8. Y. Lee and R. S. Porter, *Polym. Eng. Sci.*, **26,** 633 (1986).
9. J. P. Jog and V. M. Nadkarni, *J. Appl. Polym. Sci.*, **30,** 997 (1985).
10. D. Campbell and M. M. Qayyum, *J. Polym. Sci. Polym. Phys. Ed.*, **18,** 83 (1980).
11. A. K. Gupta, V. B. Gupta, R. H. Peters, W. G. Harland, and J. P. Berry, *J. Polym. Sci. Polym. Phys. Ed.*, **27,** 4669 (1982).
12. R. D. Icenogle, *J. Polym. Sci. Polym. Phys. Ed.*, **23,** 1369 (1985).
13. E. Martuscelli, M. Pracella, and L. Crispino, *Polymer*, **24,** 693 (1983).
14. E. J. Clark and J. D. Hoffman, *Macromolecules*, **17,** 878 (1984).

Received May 10, 1990
Accepted October 12, 1990